Chapter 18
Tsunami-Deck: A New Concept of Tsunami Vertical Evacuation System

Abdul Muhari, Fumihiko Imamura, and Shunichi Koshimura

Abstract We introduce the concept of a new type of vertical evacuation shelter. It combines the function of pedestrian bridge and tsunami tower, which are then installed at intersection. The idea provides the ease of constructing and maintenance in addition to the loss of required land acquisition. We first evaluate the performance of pedestrian bridges during the 2011 tsunami in Japan by taking into account the exposure component in term of their position from the shoreline and the susceptibility component in term of the tsunami height around the bridge as the influencing parameters in determining damage probability. We developed fragility curves to show that pedestrian bridges lay on an area less than 500 m from the coastline (around 0.1 of the maximum inundation extent), or in the area where the tsunami flow depth are 1.5 of the height of the bridge's deck have more than 50 % probability to be damaged by the tsunami. If the function of pedestrian bridge will be expanded into 'Tsunami-deck', the information about tsunami behavior at the intersection therefore becomes important. For that reason, we performed a set of numerical experiment of tsunami flow at the intersection to determine conditions that will allow the installation of tsunami-deck with a height similar to the average height of the existing pedestrian bridge. By doing so, we attempted to determine preliminary placement criteria for Tsunami-deck in order to ensure the safety of evacuee. The results gave an opportunity to have more distributed vertical evacuation shelter in flat and densely populated areas.

Keywords Tsunami-deck • Pedestrian bridge • Sudden expansion • Hydraulic gradient

---

A. Muhari (✉) • F. Imamura • S. Koshimura
International Research Center for Disaster Science (IRIDeS),
Tohoku University, Sendai, Miyagi, Japan
e-mail: aam@tsunami2.civil.tohoku.ac.jp

Y.A. Kontar et al. (eds.), *Tsunami Events and Lessons Learned: Environmental and Societal Significance*, Advances in Natural and Technological Hazards Research 35,
DOI 10.1007/978-94-007-7269-4_18,

18.1 Introduction

In pre-disaster condition, difficult to find space for vertical evacuation structures is the common problem in a densely populated area. Utilizing the existing tall buildings especially in developing countries are sometimes risky because the structural strength is not adequate against the strong ground shaking before the tsunami (e.g. Muhari et al. 2010; Imamura et al. 2012). In densely populated cities, therefore, horizontal evacuation and utilizing the natural hills (if any) is the most common option for tsunami evacuation. However, the available evacuation time starts from the occurrence of the earthquake until the first arrival of the tsunami wave is very limited. Also, some physiological aspects play an important role in determining the evacuation behavior. Experience during the 2011 East Japan tsunami demonstrated that many people returned to the tsunami affected area to pick up their relatives using cars (Muhari et al. 2012). As an implication, massive traffic jams occurred along the roads that supposed to be used for evacuation, and thus delay the people to reach safe areas. To overcome the above situations, a new type of vertical evacuation structure namely Tsunami-deck is proposed. The underlying conception is the combination of two distinct structures with different conditions and experiences as evacuation shelter in Japan. The first is the pedestrian bridge. During the 2011 tsunami in Japan, many of them were survived and used for rapid evacuation by those who get trapped in a traffic jam around the intersection (Muhari et al. 2012). However, not so many people can be accommodated due to the limited space available on the bridge's deck. The second structure is tsunami tower, but applying the tsunami tower in a populated city is difficult because it requires large open spaces for the structures. We are then thinking to utilize both structures by eliminating their weaknesses and complement their strength to develop a flexible (easy to construct and to maintain) and solution-oriented evacuation structure of the above mention evacuation problems. The limited space in pedestrian bridge is trying to be solved by expanding the deck to occupy the whole area at intersection. This means that we will have an evacuation tower at the intersection (Fig. 18.1). By doing so, several advantages are obtained such as the applicability in densely populated areas, multi-purpose in daily basis i.e. as pedestrian bridge, easy to construct and easy to maintenance, and the most important thing is that it gives an adequate temporary evacuation shelter for those who get trapped in a traffic jam during evacuation.

Since the basic idea is to extend the function of the pedestrian bridge, the limitations may come from the design height. The existing height of pedestrian bridge is around 4.5–5 m. Open structure with height taller than this might not be appropriate for the elderly in case of rapid evacuation. Therefore, criteria for its placement according to the tsunami characteristics at intersection are necessary.

We first evaluate the performance of pedestrian bridges during the 2011 tsunami in Japan. Evaluation is carried out by considering two parameters that influence the damage probability. First is the exposure in term of their position from the shoreline and the second is their susceptibility in term of the tsunami height around the bridge. Based on the developed fragility curves, we establish the placement

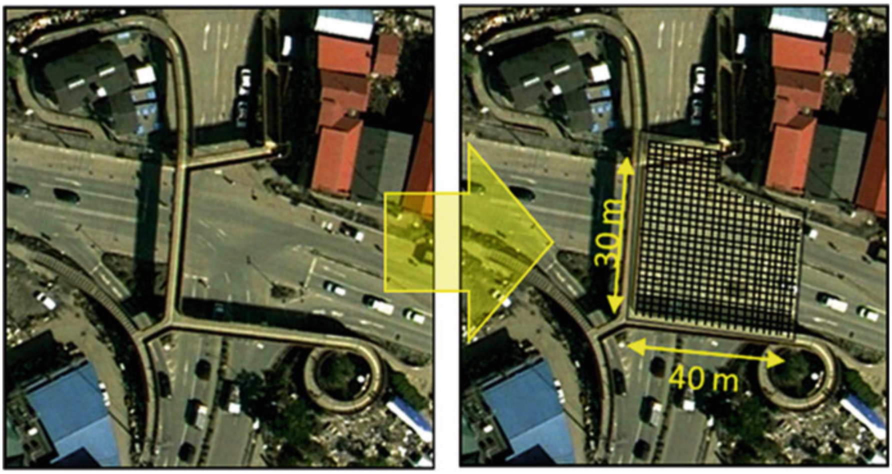

Fig. 18.1 An artist figure to describe the conception of tsunami-deck

criteria to ensure the safety of the evacuee if the tsunami-deck built to the same height as a pedestrian bridge. Starting from the concept of sudden expansion phenomena (e.g. Goto and Shuto 1983), we performed a set of numerical experiment to parameterized conditions that will allow the sudden drop of tsunami height due to the building configuration at intersection. Once the placement criteria for Tsunami-deck are established, further analysis from the structural point of view can be conducted.

18.2 Methodology

18.2.1 Fragility Curves for Pedestrian Bridge

We compiled 52 pedestrian bridges placed inside the tsunami affected areas through the visual inspection of satellite image, field survey data and utilizing the oblique photograph provided by the Geographic Survey Institute of Japan (2011). The damage levels of pedestrian bridges were then classified into three classes (see Table 18.1): (A) is heavily damaged, which described as a condition where bridges are swept away or damage on its deck, (B) is partially damage indicated by damage in the stairs or fence so it needs to be fixed before re-use, and (C) is a condition where bridges are only inundated and it can be directly used after the tsunami.

We are now analyzing the fragility of pedestrian bridge in term of their susceptibility related to tsunami flow depth around the bridge. In general, higher tsunami flow depth will increase the damage probability of the pedestrian bridge. Even though the damage might be caused by the impact of debris collision, in this study we use tsunami

Table 18.1 Damage criteria of pedestrian bridge

No	Damage classification	Indicator
1	Heavily damage (swept away)	A
2	Slight damage (i.e., stairs)	B
3	Survived (only inundated)	C

flow depth as the only observable parameter from field survey. Some of debris stranded on the bridge's stairs was visible from satellite imageries, but incomplete figures for all bridges might yield inconsistent interpretation. Therefore, debris impact is excluded from the analysis.

The cumulative damage probability is given through the widely used fragility equation (e.g. Koshimura et al. 2009) as follow,

$$P_i(x) = \Phi\left[\frac{\ln x\text{-}\mu'}{\sigma'}\right] \tag{18.1}$$

Here, P is the cumulative probability of specific damage classification (i), *Φ* is the standardized lognormal distribution function, *x* is the median of the observed tsunami flow depth, and is the mean and standard deviation of random variable of *x* respectively. In order to obtain the last two statistical parameters, we first calculate the inclination (μ_y) and intercept (σ_y through performing the least-square fitting plot of ln *x* and the inverse of lognormal distribution function Φ^{-1}. Next the mean and standard deviation were determined by ($-\mu_y/\sigma_y$) and ($1/\sigma_y$) respectively (e.g., Shoji and Moriyama, 2007).

For the fragility in term of the exposure, Eq. 18.1 is modified since the damage probability will be decreased along with the increment of the distance from the shoreline. The modification is given as follows,

$$1 - [P_i(x)] = 1 - \Phi\left[\frac{\ln x\text{-}\mu'}{\sigma'}\right] \tag{18.2}$$

By applying these equations, fragility curves for pedestrian bridges are developed and discussed in the next chapters.

18.2.2 Placement Criteria of Tsunami-Deck

In principle, the deck height should be higher than the maximum surrounding tsunami flow depth. If the buildings around the intersection withstand the tsunami, the so-called sudden expansion phenomenon where the flow depth is suddenly dropped due to the rapid change of flow direction toward different direction will be occurred depending on the building configuration at the intersection. This section will focus to elaborate the building configuration that will allow the sudden expansion phenomenon to occur.

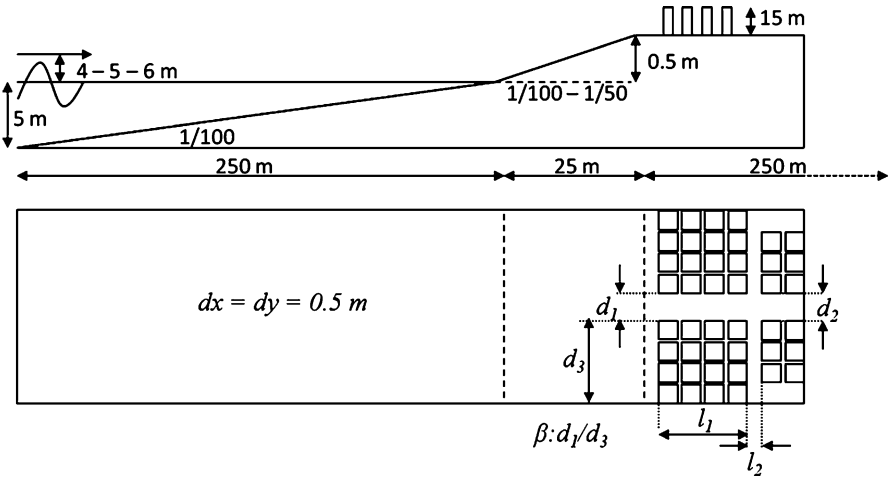

Fig. 18.2 Design of hypothetical town for numerical simulation of tsunami at intersection

Goto and Shuto (1983) analyzed factors that influence the expansion coefficient when tsunami flows along the lined obstacles. However, their works were limited in two parallel obstacles where there was no actual representation of the intersection. In this study, we perform numerical exercises using a hypothetical town that is set as shown in Fig. 18.2. Residential block prior the intersection occupied all areas, while the second is not. This design allows the flux at intersection to spread out through different direction, and minimizing the unnecessary reflecting flows from the sidewalls. In reality, this design can only able to represent areas where the width of residential block is much bigger than the width of the road between them.

A set of non-linear shallow water equation as given in Imamura (1996) is used to model the propagation and inundation of the tsunami, which is initialized by a sine wave in the ocean boundary of the domain. Goto and Shuto (1983), and Tsudaka et al. (2011) had demonstrated the reliability of 2D Shallow Water Equation (SWE) to represent flow passing through obstacles. They validated the result of numerical calculation using SWE with experimental data and obtained a good agreement. However, one should note that this approach has limitation on reproducing flood-water behind building (Tsudaka et al. 2011). Also, the absence of the momentum diffusion term in the traditional SWE might yield less accurate of modeled water level due to the lack of lateral diffusion at intersection.

We conducted the numerical exercises to assess the influence of four parameters in determining the flow characteristic at intersection. The initial sine wave – assumed as the tsunami – is set in different amplitude ranging from 2 to 6 m as shown in Table 18.2. The numerical exercises were conducted in flat (slope 0) and in sloping topography (1/100 and 1/50). In the following explanations, four parameters assessed in the numerical exercises are described. Symbols are referring to Fig. 18.2 and values of each numerical case are referring to Table 18.2.

Table 18.2 Scenarios for numerical simulation of tsunami at intersection

Case	Slope 0					Slope 1/50		Slope 1/100	
	d_2/d_1 (D)	l_1/l_2	l_2/l_1	β	Amplitude (A) (meter)	d_2/d_1 (D)	Amplitude (A) (meter)	d_2/d_1 (D)	Amplitude (A) (meter)
Case 1	1.20	5.9	0.17	0.11	2, 3, 4, 5, 6	1.20	5.00	1.20	5.00
Case 2	1.40	4.7	0.22	0.16	2, 3, 4, 5, 6	1.40	5.00	1.40	5.00
Case 3	1.60	3.5	0.27	0.21	2, 3, 4, 5, 6	1.60	5.00	1.60	5.00
Case 4	1.80	2.3	0.32	0.24	2, 3, 4, 5, 6	1.80	5.00	1.80	5.00
Case 5	2.00	–	–	0.28	2, 3, 4, 5, 6	2.00	5.00	2.00	5.00
Case 6	2.20	–	–	–	2, 3, 4, 5, 6	2.20	5.00	2.20	5.00

A. The influence of expansion ratio (*D*). This parameter is assessed by increasing the road width after the intersection (d_2) while the road width of the road before the intersection (d_1) is remaining.
B. The influence of road width parallel to the shoreline (l_2) is analyzed by increasing their width while the length of residential blocks prior the intersection (l_1) is constant.
C. The effect if some part of the houses along the road prior to the intersection were damaged by the tsunami is assessed by reducing the length of road prior to the intersection (l_1) and comparing it to the width of road that parallel to the shoreline (l_2).
D. Lastly, we estimate the effect of the ratio between the width of the road toward the intersection (d_1) and the width of residential blocks (d_3), named as beta (β) on influencing the sudden expansion at an intersection.

From the results of each scenario, a cross section at the middle of the road perpendicular to the shoreline is extracted and analyzed. The numerical exercises are conducted in a topographic domain with 0.5 m cell size. Selection of the grid size is according to an empirical relation of $dx/(g\ h_{max})^{1/2}\ T < 3\times10^{-3}$ to obtain $0.5 <$ predicted value/measured value < 2 proposed by Fujima (2012). The wave period of 0.5 h is selected for the sin wave as initial. This period is similar to the average observed period of the first wave during the 2011 Tohoku tsunami at Sendai buoys.

18.3 Results and Discussions

We classified the damage rank, cumulative frequency and cumulative damage probability in the 1-m range. In terms of their location; damage rank, cumulative frequency and cumulative damage probability were analyzed in every 250 m distance.

The regression analysis gave parameters shown in Table 18.3. There are used to determine the best fit of fragility curves in term of the exposure with the obtained

Table 18.3 Statistical parameters for fragility function obtained from regression analysis

Variable of fragility (x)	μ′	σ′	R^2
Exposure (distance from the shoreline)			
Damage classification (A)	4.12	1.53	0.74
Cummulative (A) + (B)	5.24	1.13	0.61
Susceptibility (tsunami inundation)			
Damage classification (A)	1.72	0.33	0.64
Cummulative (A) + (B)	1.20	0.42	0.81

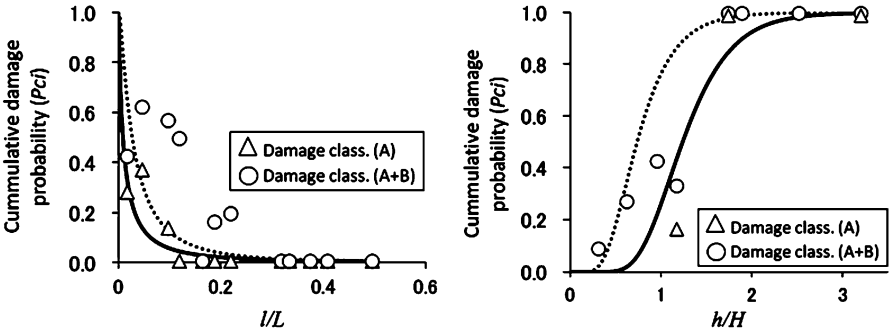

Fig. 18.3 Fragility curves for exposure (*left*) and susceptibility (*right*) parameters. *Solid line* indicates the fragility for criteria (A) and *dashed line* for cumulative (A) + (B)

coefficient correlations (R^2) as 0.74 for (A) and 0.61 for (A+B). In term of susceptibility, the coefficient correlations were obtained at 0.64 for (A) and 0.81 for (A+B).

The fragility curves are then developed by plotting the damage probability of the non-dimensional number for each fragility parameter (Fig. 18.3). The non-dimensional number for exposure is defined as the ratio between the locations of the bridge from the shore (l) with the maximum tsunami inundation distance (L), which is taken as 6 km. As for the fragility curve in term of susceptibility, the non-dimensional parameter is given by the ratio between the observed tsunami run-ups (h) to the height of the pedestrian bridge (H).

It can be seen that most of pedestrian bridges have more than 50 % probability to be damaged by tsunami if they were placed in the area up to 1.2 km from the coastline (or 0.2 of the assumed maximum inundation extent). Also, it has more than 50 % probability to be swept away by tsunami if the surrounding flow depths are 1.5 of the height of bridge's deck or around 6–7.5 m. This height of the tsunami was experienced by almost whole areas in the Sanriku coast within the distance of 0.5–1 km from the shore (Mori et al. 2011). Therefore, placement criteria for pedestrian bridge and tsunami-deck are necessary in order to fulfill the need to have evacuation facilities in the area described above.

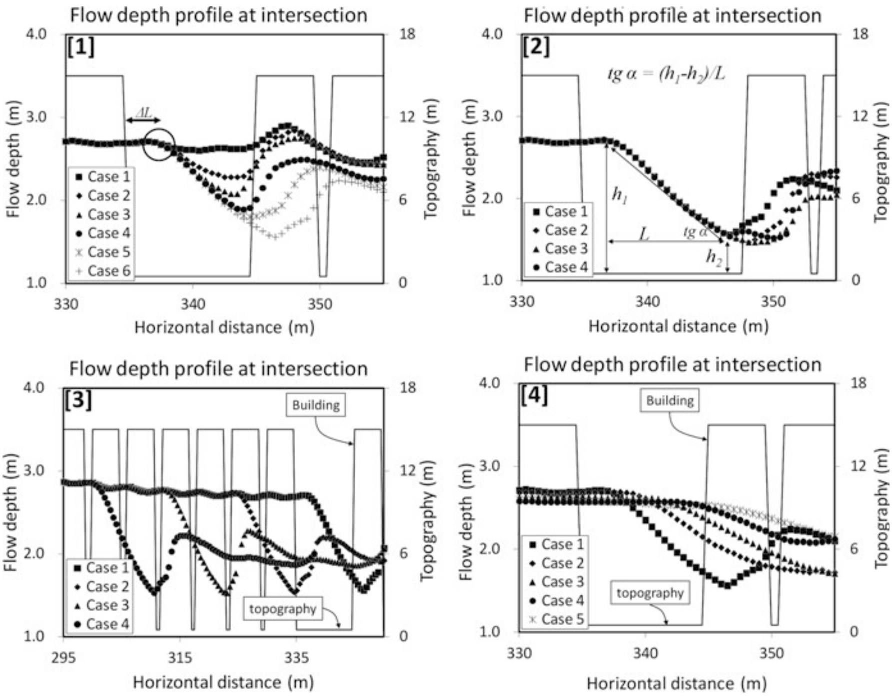

Fig. 18.4 The influence of the following parameters to the modeled water surface at intersection (refer to panel [*1*]–[*4*]): [*1*] expansion ratio (*D*), [*2*] road width parallel to the coastline (l_2), [*3*] the length of residential block (l_1) and [*4*] β (ratio between d_1 and d_2)

18.3.1 Placement Criteria for Tsunami-Deck

The dynamic features of tsunami flow at intersection might be varied depending on the geometric configuration of the junction and the surrounding building arrangement. We first analyzed the influence of expansion ratio (*D*) as given in Fig. 18.4, panel [1]. If (d_1) is relatively similar to (d_2), then the hydraulic gradient (tg α) become small (see description of tg α in Fig. 18.2, panel [2]). The tg α will start to be visible if the expansion ratio (*D*) 1.4, and saturated when *D* equal to 2.

In term of the Froude number (Fr), scenario we used in these numerical exercises brought the range of Fr as 1.13–1.34. This is higher than critical condition (Fr $>$ 1) because bore usually observed under super critical condition. By plotting the tg α with the expansion ratio (*D*) as given in Fig. 18.5 (A), we confirmed that higher Fr yields to larger hydraulic gradient at intersection. However, one should note that in a real situation, sudden expansion in high Froude number could only be observed if the surrounding building survived the tsunami.

The next analyses are taking into account the effect of road width parallel to the coastline (l_2), and the effect of road length prior to the intersection (l_1) on influencing the hydraulic gradient. Our results show that no significant effect of these factors.

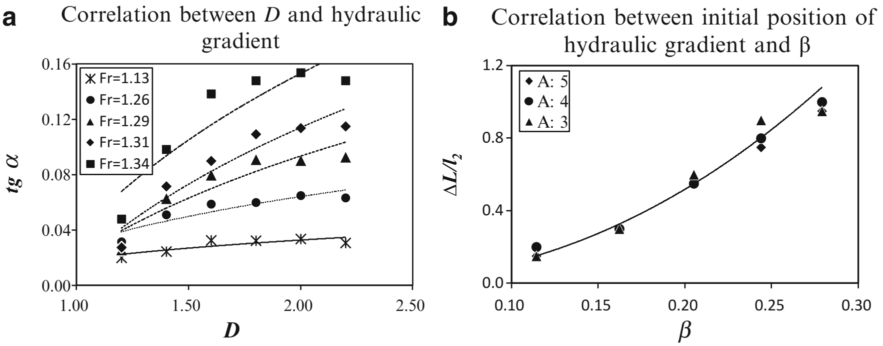

Fig. 18.5 Plotting correlation between: (**a**) expansion ratio (D) and hydraulic gradient (tg α), (**b**) correlation between the initial position of hydraulic gradient with the β

It means: first, the water mass that goes to roads parallel to the coastline will not significantly influence to the observed hydraulic gradient at the intersection. It just creates a slight difference on the initial position of hydraulic jump, which is not considered in this study (Fig. 18.4, panel [2]). Second, the length road prior to the intersection (l_1) is not influencing the hydraulic gradient. Their effect is limited only to slightly reduce the flow depth depending on the road length (Fig. 18.4, panel [3]). Therefore, one important thing to note is even if some houses along the road prior to intersection are damaged by the tsunami, the sudden expansion phenomena will still occur as long as the expansion ratio at intersection meets the requirement as discussed previously.

The influence of (β) is given in Fig. 18.4 panel [4]. It affects to determine the initial point of hydraulic gradient at intersection. Higher β will bring larger ΔL (see description of ΔL in Fig. 18.4 panel [1]). We drew the correlation between β with the non-dimensional parameter $\Delta L/l_2$. The last term indicates the ratio between initial points of hydraulic gradient from the rearmost cell of road prior to the intersection (ΔL) with the l_2. The result is imaged in Fig. 18.5 (B)–where 'A' denotes the amplitude of modeled waves–indicates that ΔL will overlap l_2 if $\beta > 0.25$ because the flow depth starts to decline when tsunami front already passed the intersection. It means there will be no hydraulic gradient observed at the intersection even if the expansion ratio meets the criteria as explained previously.

The results that describes of the influence of four parameters on determining the tsunami characteristics as we presented above only found in flat topography. We were not obtained similar results from sloping topography (1/100 and 1/50). Thus, this becomes a note that the dynamic features of tsunami flow at an intersection can only be used for consideration in determining the design height of the tsunami–deck if surrounding topography is relatively flat.

As the practical implications of the developed criteria; first, the tsunami-deck is applicable only if the predicted tsunami flow depth is lower than their height. Second, if the predicted maximum flow depth almost reaches the deck height,

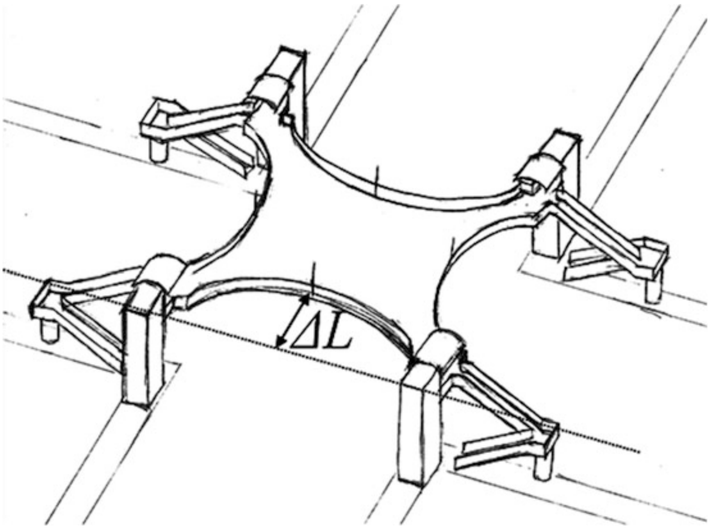

Fig. 18.6 An example of adjustment on the deck shape to accommodate the ΔL

then an adjustment should be made to the deck's design to ensure the flow passing through beneath the structure (Fig. 18.6). Also, it should be ensured that there is no source of large floating debris such as ships, boats and etc. that has possibility to strand on the tsunami-deck.

18.4 Conclusions

A new type of tsunami vertical evacuation structure is proposed to be applied in densely populated areas, especially in the developing countries. The easiness of their construction and maintenance as well as the flexibility to be put at an intersection is combined with larger accommodation space to create a reachable evacuation shelter once the traffic jam occurred during the evacuation.

As the basis for the analysis, fragility curves for pedestrian bridges are developed based on surveyed data in the tsunami affected areas along the east coast of Japan. The results indicate that pedestrian bridges placed in the area up to 1.2 km from the shore, or in the area where the estimated tsunami flow depths are 1.5 of the height of bridge's deck have a high probability to be damaged by the tsunami.

Since the above mention high risk's area might be crucial for the rapid evacuation, determining the placement criteria by using the sudden expansion phenomenon as the primary consideration solves the limitation due to the existing height. Intersections with the geometric configuration of the buildings that has $(D) > 1.5$ and $(\beta) < 0.15$ may be appropriate for tsunami deck.

The present study described only the hydrodynamic part in the introduction of tsunami-deck concept. It is highly acknowledged that the structural analysis and the potential of solid debris impact should be taken into account for the further study, which is now currently on going.

Acknowledgements We express our deep appreciation to JST-JICA project (Multidisciplinary hazard reduction from earthquakes and volcanoes in Indonesia) group 3, and the Ministry of Education, Culture, Sports, Science and Technology (MEXT) Japan for financial support through the study No.(22241042).

References

Fujima F (2012) Numerical simulation of the 2011 Tohoku tsunami in Miyako Bay, abstract for the Asian Oceania Geosciences Society (AOGS). Singapore, August 2012

Geospatial Information Authority of Japan (GSI) (2011) Information on Tohoku earthquake, available at http://www.gsi.go.jp/BOUSAI/h23_tohoku.html. Last access March 2012

Goto C, Shuto N (1983) In: Iida K, Iwasaki T (eds) Effect of large obstacle on tsunami inundation, Tsunamis–their science and engineering. Terra Scientific Publishing Company, Tokyo, pp 511–525

Imamura F (1996) Review of tsunami simulation with a finite difference method. In: Yeh H, Liu P, Synolakis C (eds) Long wave runup models. World Scientific, Singapore, pp 25–42

Imamura F, Muhari A, Erick M, Pradono MH, Post J, Sugimoto M (2012) Tsunami disaster mitigation by integrating comprehensive countermeasures in Padang city, Indonesia. J Disaster Res 7(1):48–64

Koshimura S, Oie T, Yanagisawa H, Imamura F (2009) Developing fragility function for tsunami damage estimation using numerical model and post-tsunami data from Banda Aceh, Indonesia. Coast Eng J 51(3):243–273

Mori N, Takahashi T, Yasuda T, Yanagisawa H (2011) Survey of 2011 Tohoku earthquake tsunami inundation and run-up. Geophys Res Lett 38:L00G14. doi:10.1029/2011GL049210

Muhari A, Imamura F, Natawidjaja DH, Post J, Latief H, Ismail FA (2010) Tsunami mitigation efforts with pTA in West Sumatra Province, Indonesia. J Earthq Tsunami 4(4):341–368

Muhari A, Koshimura S, Imamura F (2012) Performance evaluation of pedestrian bridge as vertical evacuation during the 2011 tsunami in Japan. J Natur Disaster Sci 34(1):79–90

Shoji G, Moriyama T (2007) Evaluation of the structural fragility of a bridge structure subjected to tsunami wave load. J Nat Disaster Sci 29(2):73–81

Tsudaka R, Shigihara Y, Fujima K (2011) Accuracy of tsunami numerical simulation with high-resolution topographic data. XXV IUGG General Assembly. International Association of Seismology and Physics of the Earth's Interior, Melbourne, 28 June–7 July, 2011